Simulation of an Integrated UTC-Photodiode with a High-Speed TIA for 5G mm-Wave Generation

Dimitrios Konstantinou*†‡, Christophe Caillaud†, Tanjil Shivan‡, Simon Rommel*,
Ulf Johannsen*, Fabrice Blache†, Franck Mallecot†, Viktor Krozer‡, and Idelfonso Tafur Monroy*

*Eindhoven University of Technology, 5600MB Eindhoven, Netherlands
†III-V Lab, a joint Lab from Nokia, Thales and CEA, 91767 Palaiseau Cedex, France
‡Ferdinand-Braun-Institut, Leibniz-Institut für Höchstfrequenztechnik (FBH), 12489 Berlin, Germany
Email: d.konstantinou@tue.nl

Abstract—This work introduces a subsystem level co-simulation for generation, boosting and transmission of millimeter wave signals for 5G applications. The simulation processes to model the full equivalent circuit of uni-traveling carrier photodiodes based on reflection coefficient measurements are analyzed. The optoelectronic lumped equivalent is co-integrated with a transimpedance amplifier design synthesized by high speed transistors. The proposed broadband component achieves competitive performance characteristics exhibiting high gain.

Index Terms—UTC-PD, TIA, mm-waves, 5G technology.

I. INTRODUCTION

In the advanced era of 5G, the infrastructure of future communication networks will provide advancements to telecommunication services offering broadband connectivity to a large number of users. An efficient way to provide these connections are hybrid optical-wireless links operating in the lightly licensed millimeter wave (mm-wave) bands allowing for larger bandwidth 5G new radio (5G NR) signals [1]. Figure 1, illustrates a unit where photonics and RF electronics convergence is maximized. This interface entails a uni-traveling carrier photodiode (UTC-PD) where optical signals are converted to mm-waves, a transimpedance amplifier (TIA) and a transmitting antenna. This paper presents the techniques for acquiring the equivalent circuit of UTC-PDs. Moreover, the high transimpedance gain capabilities of a broadband TIA are simulated. Finally, the co-integration effects by implementing wirebonding between the TIA and a UTC-PD are discussed focusing on the significance of the wirebond length to the bandwidth of the device.

II. EQUIVALENT CIRCUIT MODEL OF UTC PHOTODIODES

UTC-PDs have high sensitivity, broad bandwidth and high saturation power due to the unidirectional motion of electrons (as the only active carriers) within the intrinsic region of the device [2]. To characterize the important aspects of UTC-PDs and perform a thorough analysis of their characteristics, the extraction of their corresponding RC circuit is essential. The synthesis of the equivalent circuit, shown in Fig. 2a), is
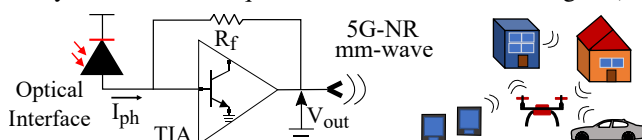

Fig. 1. A mm-wave transmission component combining a UTC-PD, a TIA and an antenna element transmitting 5G-NR based signals to various end-users.

divided in three major steps. First, the waveguide connected to the active region of the photodiode is simulated based on reflection coefficient measurements of short (SC) and open (OC) on-wafer structures. Then, the junction capacitance (C_j) and series resistance (R_s) of the UTC-PD are extracted from the S_{11} parameters. Finally, through bandwidth (S_{21}^{PD}) measurements, the electron transit time circuit is derived and linked to the S_{11}-based equivalent via an adjusting block.

A. Waveguide Modeling

By acquiring the reflection coefficient data with a VNA, the magnitudes of the waveguide parameters can be extracted analytically, or by using lumped components and numerical optimization (e.g., in ADS). The short circuit structure has an inductive behavior and therefore the measured waveguide S_{11}^{WG} parameters can be matched with an inductor (L_{WG}). The same process models the open circuit that has a capacitance (C_{WG}). Moreover, a resistor ($R_{//}$) is added in series to C_{WG} to correct for the non-ideal performance of the open structure (e.g. potential leakage to substrate). In some cases $R_{//}$ is small and can be omitted. Furthermore, analytical methods provide the magnitude for both $C_{WG} = 1/(j\omega Z_{OC})$ and $L_{WG} = Z_{SC}/(j\omega)$ with very good precision once the impedances of the short (Z_{SC}) and open (Z_{OC}) structures are calculated.

B. Extraction of C_j and R_s of the active region in UTC-PDs

The properties of the waveguides connecting the photodiode to the external world are important, as they can affect the response. After obtaining these parameters, the junction capacitance and series resistance are assessed. C_j depends on the size of the intrinsic region within the diode and R_s stems from the resistive contacts between its different semiconductor layers. For the parametric estimation of these elements, the S_{11}^{PD} data of the measured diodes are inserted in ADS and the optimization process calculates the two unknown elements (i.e., R_s and C_j). To achieve the optimal matching between the measurements and the circuit model, a shunt resistor R_{Shunt} is connected in parallel to C_j. R_{Shunt} is high (range of $k\Omega$) and in the majority of the simulations the parallel branch is considered as open. Alternatively, these elements can be directly derived from the asymptotic behavior of the S_{11}^{PD} [3].

C. Electron Transit Time Equivalent

The bandwidth of the S_{11}-based equivalent is very high and it does not match with the experimental S_{21}^{PD} parameter
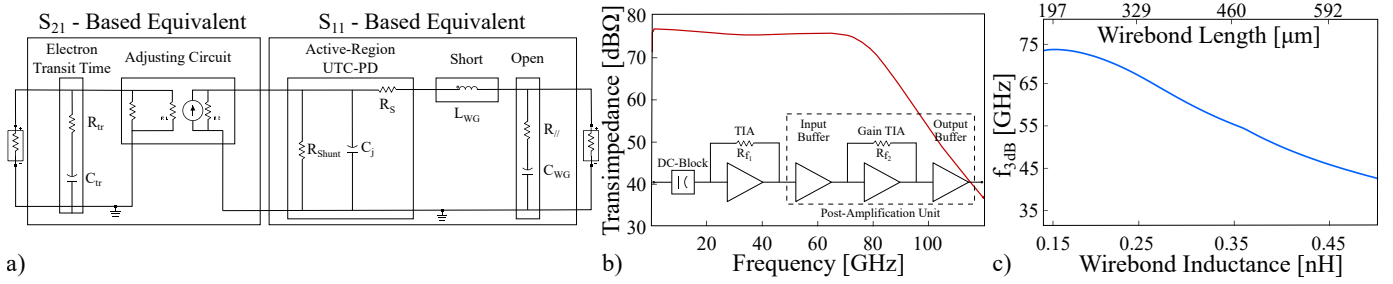
Fig. 2. a) Full equivalent circuit of a UTC-PD; b) block diagram and transimpedance of the TIA; c) 3dB-Bandwidth of the mm-wave device.

measurements. This is due to the fact that the bandwidth of a photodiode is based on both the RC-time constant (τ_{RC}) of the device as well as the transit time (τ_{tr}) of the majority carriers (electrons) through the junction. Thus, the transit time can be approximated as an additional RC cut-off time [4]. The values of the lumped elements R_{tr} and C_{tr} are evaluated based on the experimental S_{21}^{PD} curves. In addition, an adjusting circuit capable of adapting the amplitude of the imported S_{21}^{PD} parameters without changing any of the properties of the measured curve interfaces the two equivalents of the UTC-PD. Using this S_{21} equivalent, a UTC-PD can be fully modeled with lumped circuit elements while perfect matching between measurements and simulations is achieved with an error percentage calculated below 5 % for all the abovementioned described processes.

III. SIMULATION OF A MM-WAVE TRANSMITTER

A. A High Gain TIA Operating in V-band

The generated mm-waves at the output of the UTC-PD require amplification in order to be transmitted to the 5G end-users. A broadband transimpedance amplifier is a suitable candidate for achieving this goal. Figure 2b) depicts a block diagram of the simulated TIA design. A DC-block at the input, prohibiting the reverse flow of DC current towards the UTC-PD, is followed by a TIA. A post-amplification unit after the TIA further increases the gain. It consists of an input buffer, a second transimpedance gain stage and an output buffer to drive the mm-wave transmitting antenna. The amplifier circuit architecture fulfils the principle of interstage impedance mismatch where a transimpedance stage (TIS) is linked to a transadmittance stage (TAS), maximizing the bandwidth of the device [5]. The TIA is based on the FBH transferred-substrate InP-DHBT technology combining single and double finger transitors with 500 nm emitter width [6]. As shown in Fig. 2b), the simulated TIA achieves a high transimpedance (>75 dBΩ) with a 3 dB-bandwidth covering the V-band ($f_{3dB} >75$ GHz). The circuit terminated to $50\,\Omega$ at both ends exhibits a gain of 34 dB and a high output saturation power of 10 dBm. The performance characteristics of this device offer a compelling solution able to amplify the mm-waves produced by UTC-PDs.

B. Optoelectronic Co-Integration

The proposed TIA is co-simulated with the equivalent circuit of a measured $4 \times 15\,\mu m^2$ waveguide UTC photodiode from III-V Lab with a responsivity 0.79 A/W and 55 GHz of bandwidth. This UTC-PD with $C_j = 24.2$ fF and $R_s = 24.3\,\Omega$ is interfaced with the amplifier through a wirebond modeled as a lumped inductor. In Fig. 2c), the inductance of the wirebond

(L_{WB}) is swept over a range of different values in order to analyze its impact on the f_{3dB} of the device. Also, in the upper x-axis of the diagram the length of a straight gold wirebond is calculated with an assumed diameter of 17.78 μm [7]. With $L_{WB} = 0.15$ nH (197 μm), the maximum f_{3dB} is obtained (73.1 GHz) where the effect of gain peaking on the response of the component is observed. Hence, the poles originating from the DC-block and the parasitic capacitances of the UTC-PD reducing the f_{3dB} are compensated by the inductance of the wirebond [8]. Thus, the co-integration does not significantly limit the frequency performance of the mm-wave transmitter.

IV. CONCLUSION

In this paper, the simulation results of an optoelectronic mm-wave transmitter capable of generating and amplifying 5G NR signals to various end-users are presented. An equivalent circuit model of uni-traveling carrier photodiodes is proposed including the effect of carrier transit time and the RC-time constant. In addition, a simulated TIA design based on InP/InGaAs HBT technology is reported operating in a frequency range including V-band is achieved exhibiting high gain and high output powers. Finally, the wirebond between a real UTC-PD and the TIA is found to not introduce significant performance degradation, making the proposed co-integrated mm-wave transmitter an ideal choice for mm-wave signals.

REFERENCES

[1] S. Rommel *et al.*, "High-Capacity 5G Fronthaul Networks Based on Optical Space Division Multiplexing," *IEEE Trans. Broadcasting*, vol. 65, no. 2, pp. 434–443, Jun. 2019.

[2] M. Achouche *et al.*, "High performance evanescent edge coupled waveguide unitraveling-carrier photodiodes for $>$40-gb/s optical receivers," *IEEE Photon. Technol. Lett.*, vol. 16, no. 2, pp. 584–586, 2004.

[3] C. Fritsche *et al.*, "Large-signal PIN diode model for ultra-fast photodetectors," in *2005 EuMC*, vol. 2, 2005, pp. 4 pp.–1218.

[4] Gang Wang *et al.*, "A time-delay equivalent-circuit model of ultrafast p-i-n photodiodes," *IEEE Trans. Microw. Theory Tech.*, vol. 51, no. 4, pp. 1227–1233, Apr. 2003.

[5] H. M. Rein *et al.*, "Design considerations for very-high-speed Si-bipolar IC's operating up to 50 Gb/s," *IEEE J. Solid-State Circuits*, vol. 31, no. 8, pp. 1076–1090, Aug. 1996.

[6] T. Shivan *et al.*, "A 175 GHz Bandwidth High Linearity Distributed Amplifier in 500 nm InP DHBT Technology," in *2019 IEEE MTT-S International Microwave Symposium (IMS)*, 2019, pp. 1253–1256.

[7] X. Qi *et al.*, "A fast 3D modeling approach to electrical parameters extraction of bonding wires for RF circuits," *IEEE Trans. Adv. Packag.*, vol. 23, no. 3, pp. 480–488, Aug. 2000.

[8] G. Chen *et al.*, "Bandwidth improvement for germanium photodetector using wire bonding technology," *Optics express*, vol. 23, Oct. 2015.